ORIGINAL PAPER

Development of corrector magnet power supply for high energy photon source

Han Chao[1] · Long Fengli[1,2] · Gao Yao[1] · Wei Pengfei[1] · Liu Yuting[1] · Guo Xiaoling[1] · Chen Suying[1] · Du Yunze[1]

Abstract

Purpose High Energy Photon Source (HEPS) requires high quality, high energy beam and ultra-low emittance of 0.1 nm·rad, which puts forward high demand for power supply. In this paper, a high-performance corrector magnet power supply is developed to calibrate and adjust beam track within a certain bandwidth range to ensure the stability of beam track.

Methods The prototype of power supply adopts the new "One control Two" control mode, which adjusts the performance of two power supplies simultaneously based on digital control.

Results The experimental results show that the stability of the power supply is lower than 20 ppm, which is far better than the design index. Voltage ripple is less than 10 mV, and other performance indexes meet the physical design requirements, which can well meet the requirements of HEPS construction.

Conclusions After a lot of experiments and tests, all the parameters passed the design indicators. The successful development of this power supply has laid a foundation for the successful application of HEPS.

Keywords HEPS · Corrector power supply · Stability · Voltage ripple

High Energy Photon Source (HEPS) is one of the ten major scientific and technological infrastructures determined to be constructed in the "13th Five-Year Plan" for the national major scientific and technological infrastructure construction, and it is an important support platform for original and groundbreaking innovative research in basic and engineering sciences. The construction of HEPS will significantly improve the quality of the light and will significantly narrow the gap between China and international advanced light sources and bring China into the ranks of the world's advanced level [1–6]. Meanwhile, the construction will provide a unique and powerful support for research fields related to national security and industrial core innovation capabilities. HEPS is a high-performance light source with electron energy of 6 GeV and emittance less than or equal to 0.06 nm-rad, mainly composed of gas pedal, beamline and experimental station. As a fourth-generation photon light source, HEPS is the first high-energy photon light source in China, with the world's highest spectral brightness (10^{22} phs/s/mm^2/mrad^2/0.1%BW), higher than existing and under construction light sources in the world [7–12].

The power supply system in the HEPS project mainly includes two major parts: the booster power supply system and the storage ring power supply system. The high quality and high energy beam current requirements of HEPS and the ultra-low emittance demand make high requirements for power supply stability, ripple and other indicators in the process of physical design [13–15]. The ordinary correction magnet power supply, as an auxiliary power supply to the main magnet power supply, can correct and adjust the beam track within a certain bandwidth to ensure the stability of the beam track. To ensure the reliability and stability of future HEPS operation, a prototype correction magnet power supply was developed. The prototype adopts a new "one control two" scheme, which can not only greatly save control resources, but also can save chassis space.

Power supply parameters design

The corrector power supply prototype designed is ± 19A/ ± 12 V, and its main design specifications are listed in Table 1.

✉ Han Chao
hctc138@163.com

1 Institution of High Energy Physics, Chinese Academy of Sciences, Beijing 100049, China

2 University of Chinese Academy of Sciences, Beijing 100049, China

Table 1 Main parameters of correct power supply

Parameters	Value
Output current, A	± 19
Output voltage, V	± 12
Current stability, ppm	100 (< 8 h)
Current accuracy, ppm	100
Current repetitive, ppm	100
Voltage ripple	> 10A: Vp-p $\leq$ 100 mV(20 MHz) $\leq$ 1 kHz: $V_{rms} \leq$ 5 mV > 1 kHz: $V_{rms} \leq$ 10 mV $\leq$ 10A: Vp-p $< =$ 100 m(20 MHz) $\leq$ 1 kHz: $V_{rms} \leq$ 2 mV > 1 kHz: $V_{rms} \leq$ 10 mV

In the HEPS formal project, as many as 1000 power supplies of the same type [11]. In order to meet the reliability of future operation continuity, the reliability and maintainability of the power supply must be considered in the design phase, while for different power of the same type of power supply, the design process also needs to consider the flexibility and adjustability.

Power topological structure

The power supply topology is designed with a front-stage DC source and a back-stage H-bridge inverter with a switching frequency of 50 kHz. In order to improve the flexibility and reliability, the DC source adopts a modular design. The input 220 V AC of DC source is converted into DC power through EMI filtering, full-wave rectification, PFC power factor correction, and half-bridge rectification and filtering. The design structure of the DC source ensures the low voltage ripple of the front stage, and the output avoids the use of large-capacity filter capacitors, which can greatly save the design space. Due to the low output voltage ripple of the pre-stage DC source, the power supply does not use a voltage loop, but only a single-loop feedback mode with current feedback. The rated power of the power supply prototype is 228 W, and the DC source power design is 24 V/15A. The single power supply adopts an all-digital plus all-switch control structure, and the design scheme is shown in Fig. 1.

The key to the design of the power supply prototype structure design lies in the "one control two", that is, the two power supplies of the same specification and model are integrated in a chassis, the power part is isolated from each other, the control part is the same digital controller. The closed-loop system controls two power supplies respectively, and the whole power supply design scheme is shown in Fig. 2.
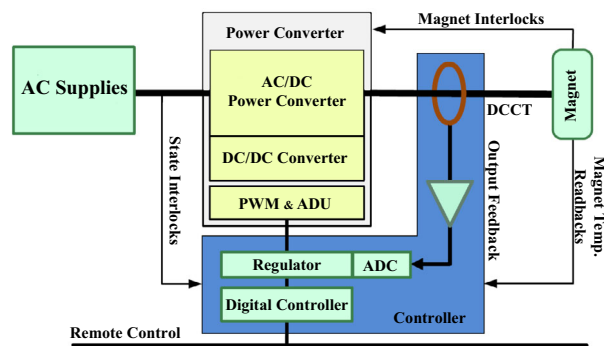
Fig. 1 The DC power supply design scheme

Power control scheme

The power supply prototype design "one control two" structure is to use a digital controller to control two power supplies, respectively, and the two power supplies operate independently of each other, without interference. The power supply system adopts the classical H-bridge topology, and the drive signal adopts the full-bridge bipolar PWM modulation. The controller generates two groups of PWM signals to control the two power supplies respectively, each group of PWM signals is output through an isolated chip, and the two groups are independent of each other. The data of the two power supplies are controlled by different PI controllers in the FPGA, and the PI parameters are determined according to the output loads of the respective power supply. The control structure is shown in Fig. 3.

The power supply prototype controller motherboard is designed with a variety of communication interfaces such as optical fiber, USB serial port and network port to meet the different modes of remote control. At the same time, in order to reduce the signal interference in the feedback loop, a current-type DCCT is used in the current closed loop, and the conversion of the output current to voltage is as close as possible to the AD sampling terminal, which further reduces the environmental interference.

The stability of the power supply mainly includes short-term stability and long-term stability. The short-term stability error is mainly caused by factors such as current ripple, which is generally related to the hardware design and can be improved by adjusting the PI parameters. The long-term stability error is mainly caused by factors such as temperature drift of the power supply, such as changes in device parameters caused by changes in temperature. In order to reduce the change in long-term stability caused by temperature change, the key components affecting temperature performance in the
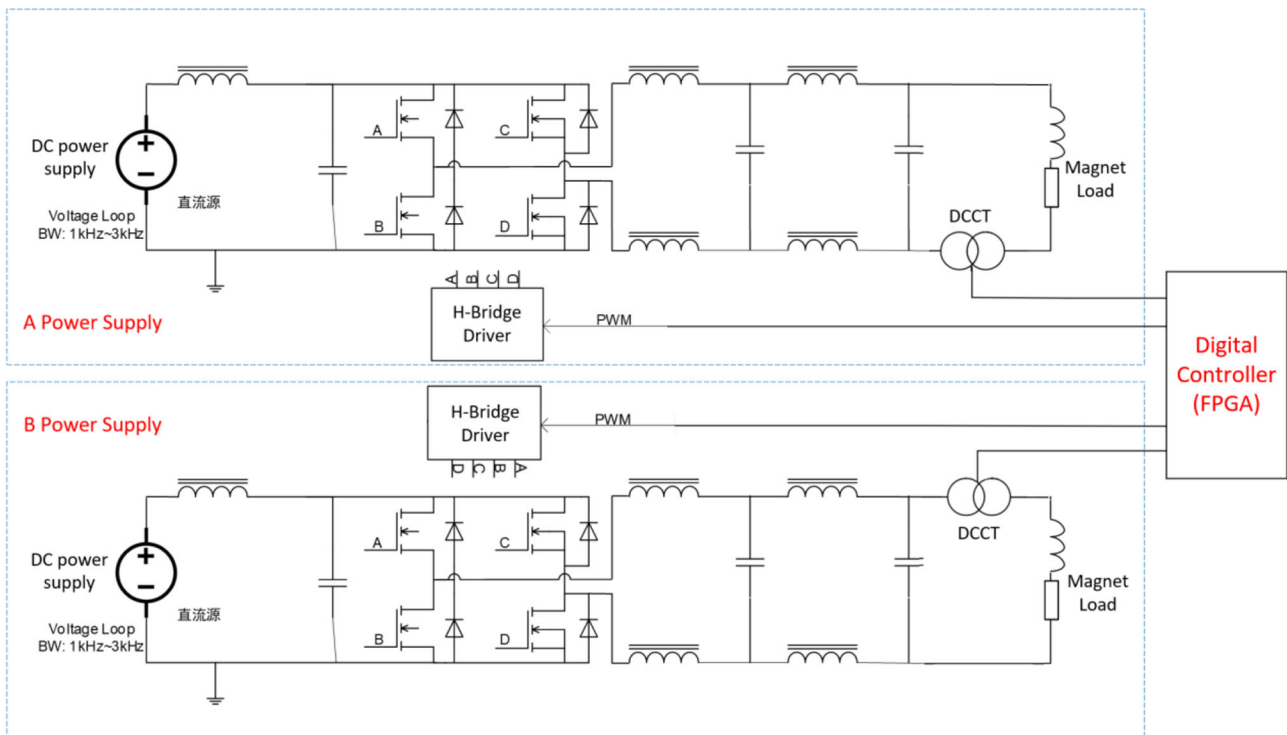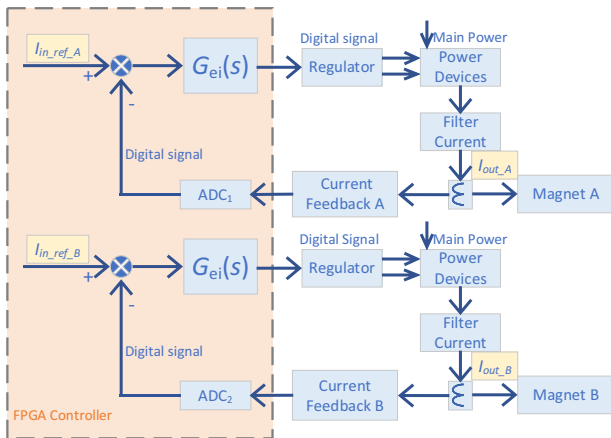
Fig. 2 The power supply prototype design scheme

Fig. 3 The power supply prototype control structure

Fig. 4 The controller mainboard structure diagram

power supply feedback loop adopt temperature compensated and thermostatically controlled. In the IV conversion design, a temperature coefficient compensation method is adopted, i.e., a paired resistor of "one positive and one negative" is used to reduce the resistance change caused by temperature change. In order to reduce the influence of temperature on the ADC, constant thermostat control is carried out on the AD sampling part. Through testing, the accuracy of thermostat control can reach 0.1°C. The main board structure of the controller is shown in Fig. 4.
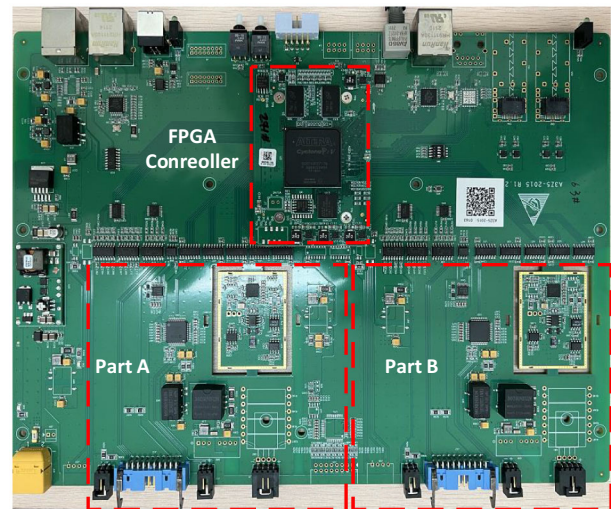
Experiment and test results

Due to the special structure of "one control two", the control board of the developed prototype adopts the scheme of directly designing the backplane on the control board instead of the traditional separate and independent design structure, which not only can save the installation space, but also reduce

Fig. 5 Corrector magnet power supply prototype

Table 2 Current long term test result

Current (A)	Stability ($\times 10^{-6}$, ppm)
2	10.9
10	13.7
19	17.7
− 2	7.4
− 10	11.4
− 19	15.3

the transmission distance of the voltage signal, which can further reduce the space interference of the power supply. The power supply prototype adopts an air-cooled heat dissipation method. The chassis is designed with a 3U structure. It is divided into two layers, the front and the back, and the middle is separated by a steel plate. One layer is mainly the power part, and the other layer is the control part. The communication between the layers is connected by interfaces and signal lines, which is not only conducive to the control of space temperature, but also can further reduce the space interference of power devices. The 3U chassis-type structure of the power supply design adopts an air-cooled cooling method to maintain the temperature in the chassis. The power supply prototype is shown in Fig. 5.

Long-term stability

In order to ensure that the current stability at each operating point can meet the stability requirements, it is necessary to record the output current value continuously for 8 h after the power supply is turned on for 30 min and warm up. The stability of the power supply at $\pm 10\%$, $\pm 50\%$, $\pm 100\%$ of the working current is recorded, respectively, and the stability calculation formula is as follows:

$$I_{stability} = \left| \frac{I - I_{avg}}{I_N} \right|_{\max} \tag{1}$$

where I_N is the rated current value, I_{avg} is the average value of the output current in a certain time, and I is the measured
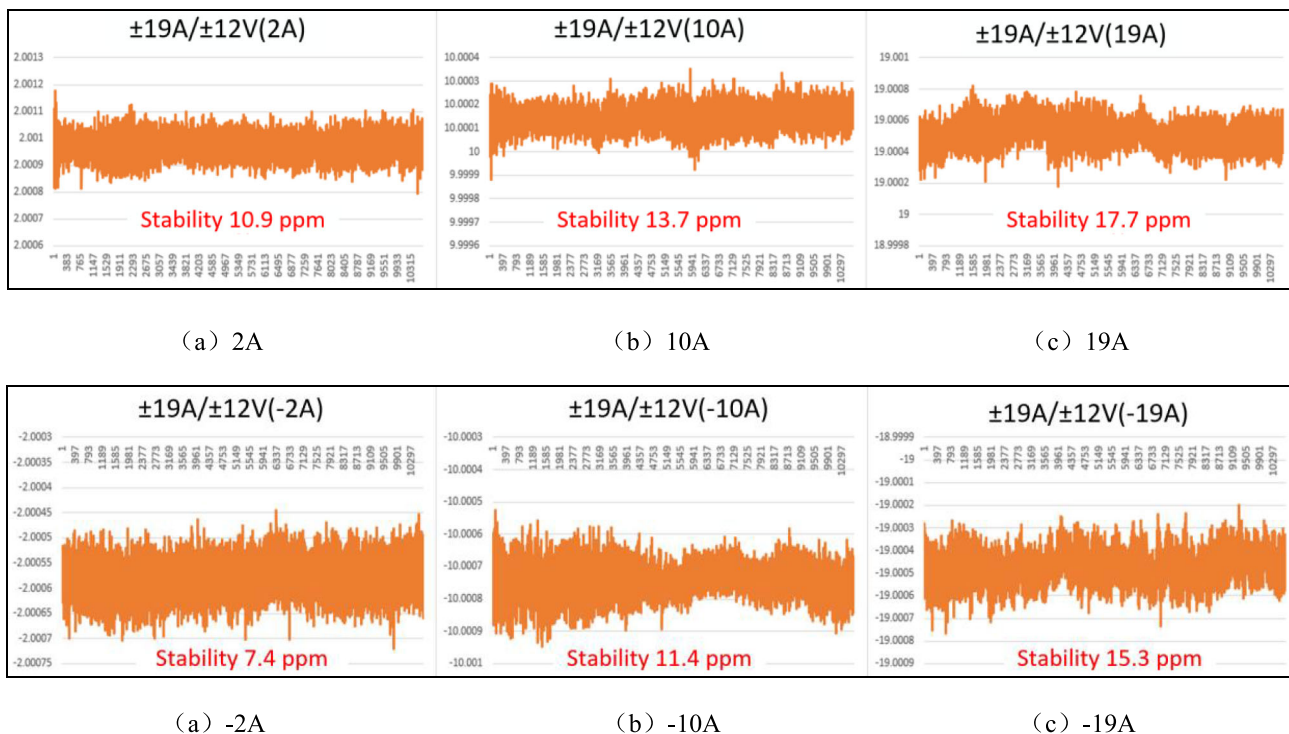

（a）2A　　　　　　　　（b）10A　　　　　　　　（c）19A

（a）-2A　　　　　　　　（b）-10A　　　　　　　　（c）-19A

Fig. 6 Current long-term test curve

Table 3 power supply accuracy test result

Set value (A)	Measured (A)	Accuracy ($\times 10^{-6}$, ppm)
2	1.999504	26.1
10	9.999753	13
19	18.999292	37.3
-2	-1.999212	41.5
-10	-9.999341	34.7
-19	-18.999495	26.6

current value. The calculation formula is the latest calculation formula according to the physical requirements. The test results are shown in Fig. 6.

The stability test results obtained by Eq. (1) are shown in Table 2.

Accuracy

In order to better realize the precise control of the beam current, the physical design puts forward a requirement of 100 ppm for the accuracy of the power supply. The accuracy is mainly affected by the conversion accuracy of the feedback loop. Therefore, it is necessary to calibrate the key components of the feedback loop first, and then calculate the accuracy error through testing. The calculation formula is as follows:

$$I_{\text{accuracy}} = \left| \frac{I_{\text{avg}} - I_{\text{set}}}{I_N} \right|_{\max} \tag{2}$$

In the formula (2), I_N is the rated current value, I_{avg} is the average value of the standard DCCT for a certain period of time, and I_{set} is the set current value. Table 3 shows the power supply accuracy test results.

The test results show that the largest accuracy error of the power supply output is 41.5 ppm which is appeared at the -2A test point. The result is fully meets the design requirements.

Repeatability

The repeatability test method is to take two test points in the positive and negative directions and test, respectively. For example, the repeatability process of testing 10A is to turn off the power for 30 min, then turn it on again and increase the current up to 10A, and then measure the output current for 30 min after stabilizing for 30 min. The final measured data are averaged and recorded as $I_{\text{avg}(1)}$; then repeat the first time to obtained the average current of the second time and recorded as $I_{\text{avg}(2)}$. Repeatability can be obtained by comparing the two average values. The calculation formula is as

follows:

$$I_{r(+50\%)} = \left| \frac{I_{avg(1)} - I_{avg(2)}}{\frac{(I_{avg(1)} + I_{avg(2)})}{2}} \right| \tag{3}$$

The power supply prototype was tested for repeatability at 2A, $-$ 2A, 10A, $-$ 10A, 19A and $-$ 19A outputs and the results are shown in Fig. 7.

Table 4 shows the repeatability test results.

The test results show that the maximum repeatability occurs when the power supply current is $-$ 2A, and the repeatability error is 15.7 ppm, which fully meets the design requirements.

## Voltage ripple

1)low frequency ripple.

Low-frequency ripple refers to the voltage ripple below 1 kHz. The low-frequency ripple design index requires that it be no greater than 2 mV when current is less than or equal to 10A, and no greater than 5 mV when current is more than 10A. Figure 8 shows the test results of the power supply voltage ripple at 4 different operating points. It can be seen that the low-frequency voltage ripple is better than the design index.

The 50 Hz ripple in the low frequency ripple is caused by the 220 V@50 Hz ac power supply, while 100 Hz ripple is the double frequency ripple.

2)High frequency ripple.

High-frequency ripple refers to voltage ripple higher than 600 Hz. Figure 9 shows the test results at four different operating points. The results show that the Fourier analysis of the high-frequency ripple shows that the maximum amplitude point appears at the frequency multiplication point of the switching frequency, and its effective value is less than 3 mV, which is better than the design requirements.

It can be seen from the Fourier analysis of the high-frequency ripple that the noise distribution of the power supply is different under different currents. The maximum noise at $\pm$ 19A is 350 kHz and 400 kHz, and it is 150 kHz at $\pm$ 2A. The reason is mainly related to the output filter network of the power supply. The spurious parameters of the output filter network lead to spurious noise at different currents. Although large noise is generated at different frequency points, it meets the ripple requirements of the power supply. At the same time the actual magnet load is 9 mH ~ 12 mH, and the current value of such high frequency is basically zero. Therefore, the ripple of the power supply completely meets the design requirements of the power supply.
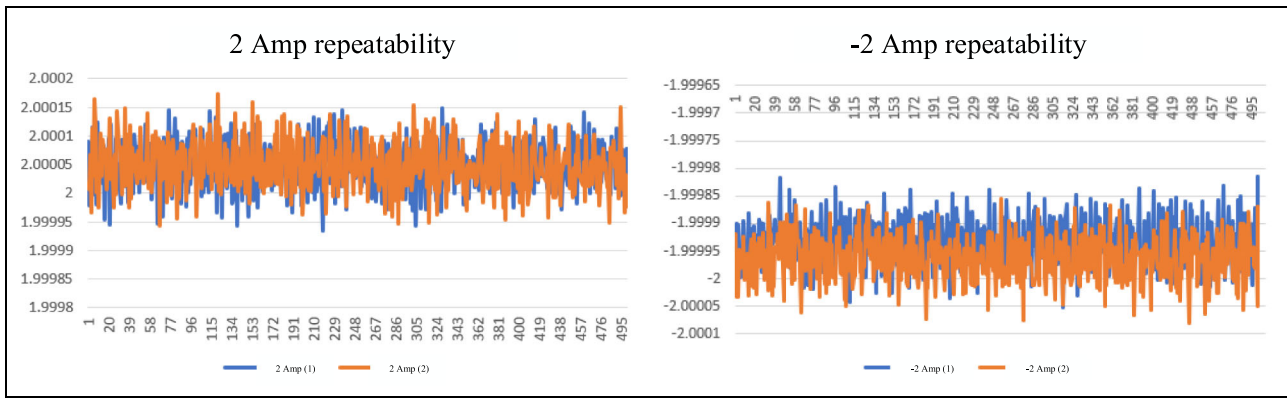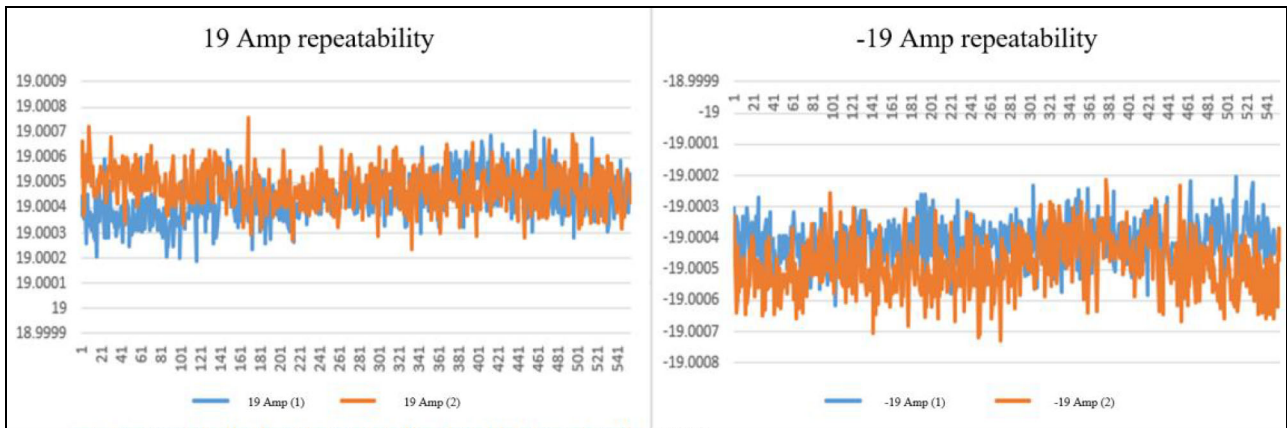
（a）2 Amp repeatability

（b）-2 Amp repeatability
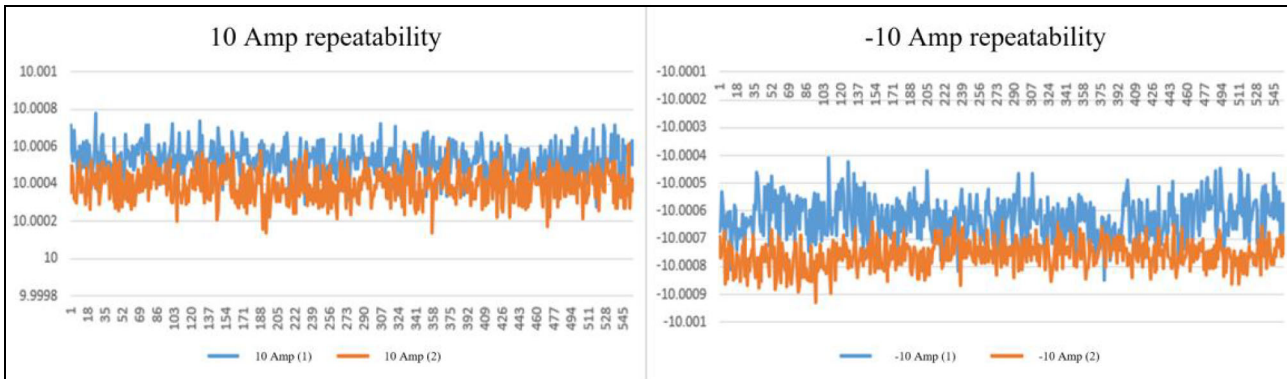
（c）10 Amp repeatability
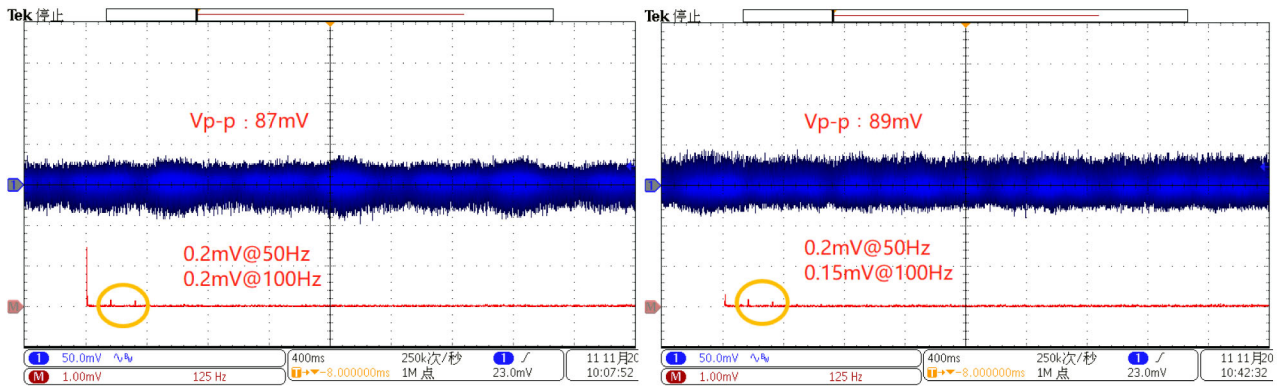
（d）-10 Amp repeatability

（e）19 Amp repeatability

（f）-19 Amp repeatability

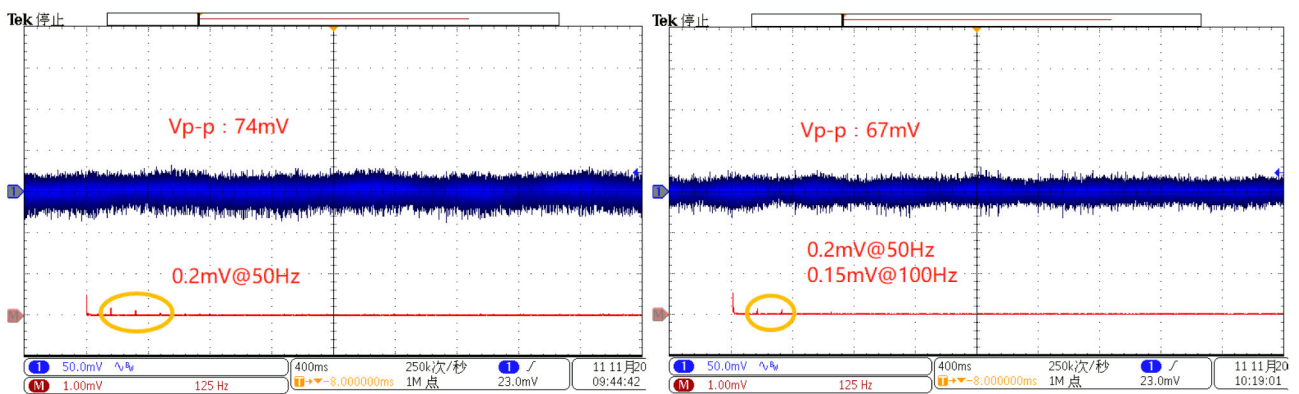**Fig. 7** Power supply repeatability test curve

Conclusion

Though the test, the performance of the developed power supply prototype meets the actual design requirements, and the prototype structure design is reasonable. Under the condition of ensuring the output performance of the power supply, the

"one control two" structure of the prototype design can not only save space, but also better save control resources, and fully meeting the performance requirements of the physical design of HEPS. Through the development of the corrector power supply prototype, the foundation has been laid for the

（a）19 Amp low frequency ripple test

（b）-19 Amp low frequency ripple test

（c）2 Amp low frequency ripple test

（d）-2 Amp low frequency ripple test

Fig. 8 Waveform of voltage low-frequency ripple

Table 4 Power supply repeatability test result

Current (A)	Repeatability ($\times 10^{-6}$, ppm)
2	0.6
− 2	15.7
10	13.2
− 10	13.0
19	2.2
− 19	3.8

batch development and application in the light source engineering construction.

（a）19 Amp high frequency ripple test

（b）-19 Amp high frequency ripple test

（c）2 Amp high frequency ripple test

（d）-2 Amp high frequency ripple test
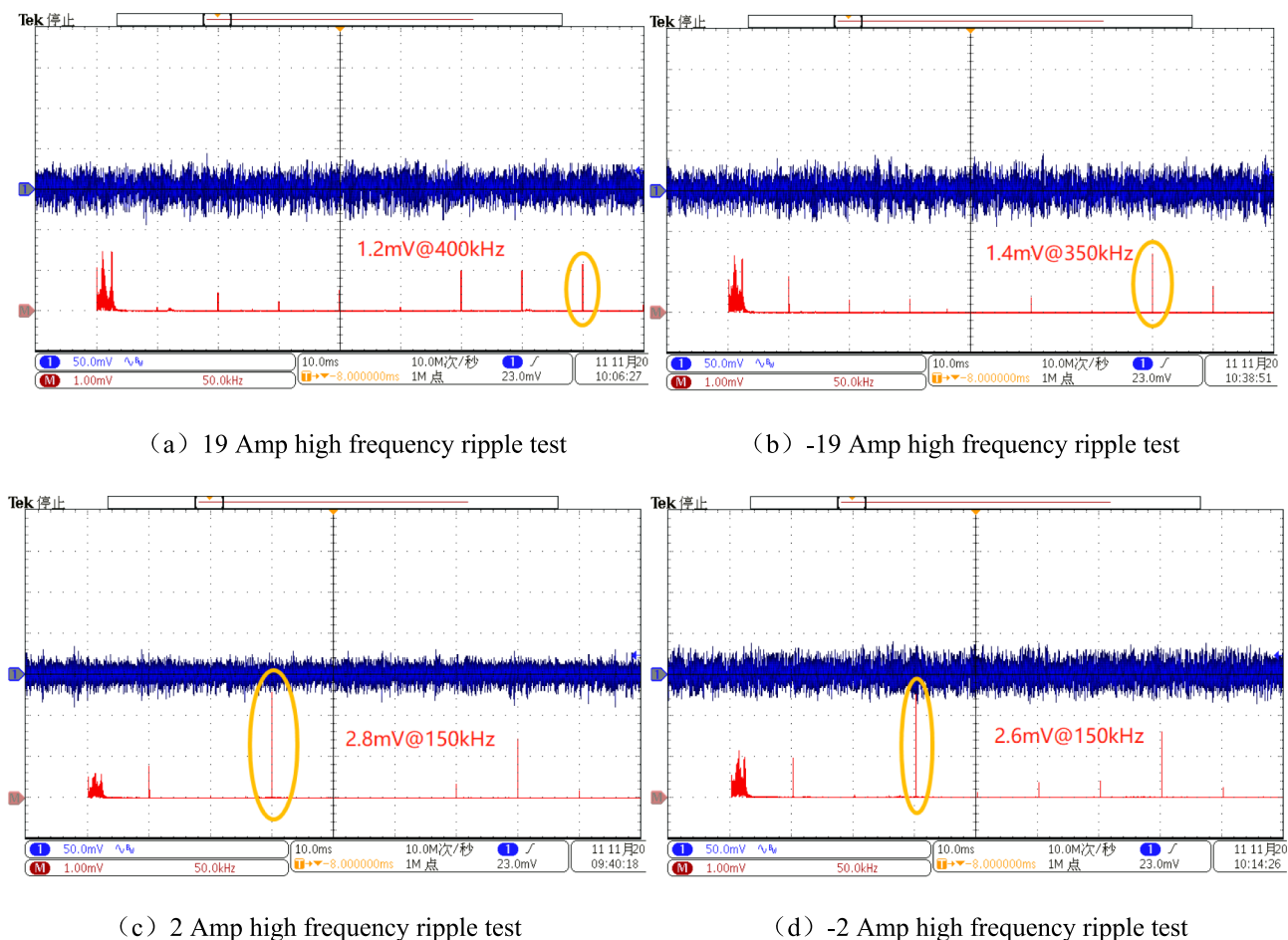
Fig. 9 Waveform of voltage high-frequency ripple

References

1. T. Fors, Unipolar Magnet PS and Precision Current Measurement R&D for the APS Upgrade[C]//ASD Seminar, November. 4, (2015)
2. M. Cerqueira. High Accuracy Current Measurement in the Main Power Converters of the Large Hadron Collider: Tutorial 53[C]//Part 53 in a series of tutorials on instrumentation and measurement, February (2014)
3. LIU Chenyao, WANG Baoshen. Dipole Power Supply for the Storage Ring of Taiwan Photon Source[C]//Proceedings of IPAC, Busan: [s.n.], (2016)
4. WANG J, DERIY B. Power supply conceptual design and R&D for the APS upgrade[C]//Proceedings of IPAC, Richmond: [s.n.], (2015)
5. W. Baosheng, L. Kuobin, L. Chenyao et al., Digital controller implementation of a corrector power converter for TPS fast corrector magnet[J]. Int. J. Inform. Electron. Eng. **7**(4), 127–131 (2014)
6. J.C.L.Brazier, *The all-digital approach to LHC power converter current control[C]//8th International Conference on Accelerator & Large Experimental Physics Control Systems,* (San Jose, Caligornia, 2001), p. 453–455
7. Liu Kuobin, Li Yida, Wang Baosheng, et al., TPS corrector magnet power converter[C]‖Proceedings of the 1th International Particle Accelerator Conference. Kyoto: [s.n.], (2010)
8. LI J Y, DONG H Y, DUAN Z, et al., Conceptual design of HEPS injector[C] // Proceedings of IPAC. Vancouver: Argonne National Laboratory, (2018)
9. XU G, CUI X H, DUAN Z, et al. Progress of lattice design and physics studies on the high energy photon source[C] // Proceedings of IPAC. Vancouver: Argonne National Laboratory, (2018)
10. DUAN Z, CHEN J H, GUO Y Y, et al. The swap-out injection scheme for the high energy photon source[C] // Proceedings of IPAC. Vancouver: Argonne National Laboratory, (2018)
11. J. Xiaoming, W. Jiuqing, Q. Qing et al., Chinese high energy photon source and the test facility[J]. Scientia Sinica Physica. Mech. Astron. **44**(10), 1075–1094 (2014). (**in Chinese**)
12. XU G, CUI X H, DUAN Z, et al. Progress of lattice design and physics studies on the high energy photon source[C]//Proceedings of IPAC, Vancouver: Argonne National Laboratory, (2018)

13. G. Xiaoling, L. Peng, H. Chao, C. Bin, Development of high precision and stability DC power supply prototype for high energy photon source[J]. Atom. Energy Sci. Technol. **53**(08), 1523–1529 (2019). (**in Chinese**)

14. L. Peng, L. Feng-li, Li. Yang, H. Chao, Design of fast corrector magnet power supply for heps storage ring [J]. Atom. Energy Sci. Technol. **54**(11), 2252–2257 (2020). (**in Chinese**)

15. S. Kun, L. Feng-li, H. Chao, Self-adaptive controller design for accelerator stabilized magnet power supply[J]. Atom. Energy Sci. Technol. **51**(06), 1116–1112 (2017). (**in Chinese**)